Multi-view People Detection on Arbitrary Ground in Real-Time [*]

Ákos Kiss[1,2] and Tamás Szirányi[1]

[1] *Distributed Events Analysis Research Group, Computer and Automation Research Institute - Hungarian Academy of Sciences, Budapest, Hungary*
[2] *Dept. of Control Engineering and Information Technology, Budapest University of Technology and Economics, Budapest, Hungary*
{kiss.akos@sztaki.mta.hu, sziranyi@sztaki.mta.hu

Keywords: multi-view detection, 3D position, projection, real-time processing

Abstract: We show a method to detect accurate 3D position of people from multiple views, regardless of the geometry of the ground. In our new method we search for intersections of 3D primitives (cones) to find positions of feet. The cones are computed by back-projecting ellipses covering feet in input images. Instead of computing complex intersection body, we use approximation to speed up intersection computing. We found that feet positions are determined accurately, and the height map of the ground can be reconstructed with small error. We compared our method to other multiview-detectors - using somewhat different test methodology -, and achieved comparable results, with the benefit of handling arbitrary ground. We also present accurately reconstructed height map of non-planar ground. Our algorithm is fast and most of steps are parallelizable, making it possibly available for smart camera systems.

1 INTRODUCTION

Single camera detecting and tracking relies on some kind of descriptors, like color, shape, and texture. However, extraordinary and occluding objects are hard to detect. Multiple cameras are often used to overcome these limitations.

In these cases, consistency of object pixels among views will signal objects in 3D space. There are many methods for finding object pixels. Using stereo cameras, the disparity map can highlight foreground, or using wide-baseline stereo imaging, image-wise foreground detection is carried out.

The resulting set of object pixels can be further segmented, and consistency check might be reduced to likely correspondent segments. This might be done using color descriptors (Mittal and Davis, 2001; Mittal and Davis, 2002), however color calibration (Jeong and Jaynes, 2008) is necessary due to different sensor properties or illumination conditions.

Foreground masks can be projected to a ground plane, and overlapping pixels mark consistent regions (Iwase and Saito, 2004). Reliability can be improved using multiple planes (Khan and Shah, 2009), or by looking for certain patterns in the projection plane

(Utasi and Benedek, 2011).

In many works authors assume known homography between views and ground plane to carry out projection. In (Havasi and Szlavik, 2011) homography parameters are estimated from co-motion statistics from multimodal input videos, eliminating the need of human supervision.

Projection of whole foreground masks is computationally expensive, but filtering pixels can reduce complexity. In some works, points associated with feet are searched, reducing foreground masks from arbitrary blobs to points and lines (Kim and Davis, 2006; Iwase and Saito, 2004).

Another gain of filtering foreground points is that - depending on the geometry - feet are less occluded than whole bodies, eliminating a great source of errors. Reducing occlusion is especially important in dense crowds, for example using top-view cameras (Eshel and Moses, 2010).

2 OVERVIEW

Our goal was to design an algorithm for detecting people in a multiview environment with possibly many views where the geometry of the ground is arbitrary, which problem is not addressed in the field.
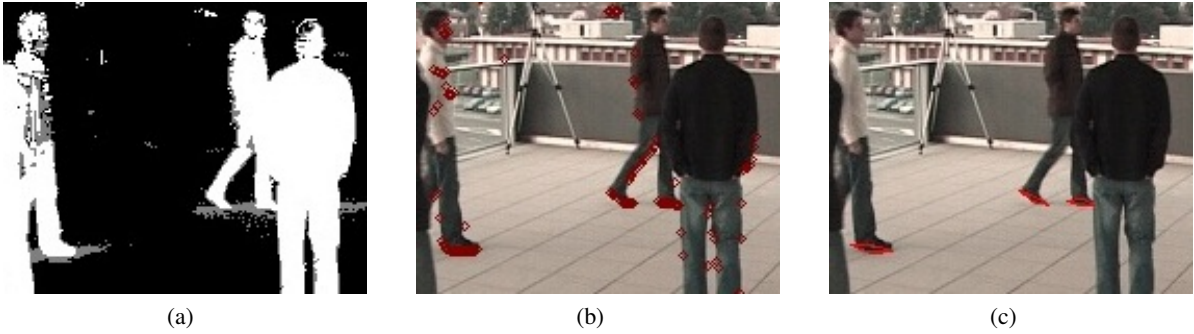

| (a) | (b) | (c) |

Figure 2: Steps of extracting ellipses covering feet: (*a*) foreground detection, (*b*) finding candidate pixel set, (*c*) forming ellipses covering these pixel sets (ellipses are visualized with lozenges).
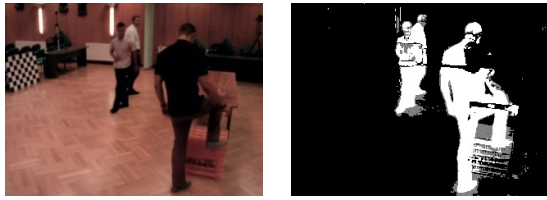

Figure 1: Shadows may corrupt foreground detection even in carefully chosen color space.

Moreover we aimed at reaching real-time running to make it available for surveillance systems.

Foreground pixels of a view correspond to lines in 3D scene space, and lines intersect in scene space at points inside the object. However, computing intersections would be slow due to large number of line pairs.

1. Number of line pairs can be decreased by filtering foreground mask. We selected candidate pixels for feet, drastically reducing number of foreground pixels.

2. We clustered candidate pixels so that clusters cover feet. These clusters are modeled with ellipses, which can be back-projected to cones in scene space. Finding intersecting cones replaces pairwise matching of lines in cluster-pairs.

Our approach has several advantages in means of both precision and speed:

- for determining cone parameters, undistortion may be carried out with few computations leading to accurate parameters,

- unlike pixels, number of clusters is proportional to number of objects regardless of image resolution,

- ground doesn't have to be flat (unlike using homographies in (Utasi and Benedek, 2011; Khan and Shah, 2009; Khan and Shah, 2006; Iwase and Saito, 2004; Berclaz et al., 2006)),

- no presumption on height range is required - which is mandatory in (Utasi and Benedek, 2011;

Khan and Shah, 2009; Khan and Shah, 2006)

On the downside:

- our algorithm may fail on incorrect foreground mask, when extracted ellipses won't cover feet precisely - as shown in Section 3.2.

- precise calibration is required for reliable estimation of cone parameters (both intrinsic and extrinsic parameters of the camera).

We show applied preprocessing steps to form ellipses from foreground mask in section 3. Section 4 introduces steps of forming cones in scene space and matching these cones. Section 5 describes feet detection from cone matches as well as details of height map reconstruction. We show results and comparison to state of the art methods in Section 6 and conclude our work in Section 7.

3 PREPROCESSING

We used a modified version of the foreground detector described in (Benedek and Szirányi, 2008) by adding white balance compensation to the model. This reduced artifacts due to self-adjustment of camera.

We filtered out small areas (less than 7px in our experiments) from the foreground mask to suppress noise - different threshold might be best for different videos.

We tried several color spaces, eliminating shadows and reflections on the ground was most reliable in XYZ color space. We used this in our experiments, however, in certain situations foreground mask was still corrupt, Fig 1 shows an example.

3.1 Filtering feet from foreground mask

Assuming camera is in upright position, pixels of feet

Figure 3: Candidate pixels can appear on arms or on foreground artifacts, and also cones corresponding to different feet can intersect.

are bottom pixels of vertical lines in the foreground mask. We call these candidate pixels. A sample of extracted candidate pixels can be seen in Fig 2(b).

Candidate pixels are usually not adjacent, because of noise and steep edges. None of these depend on image resolution, distance threshold is chosen according to image quality. In our case, we connected pixels closer than 3px to form clusters.

This makes our algorithm robust to image resolution, as increasing resolution results in more candidate pixels, but the same number of clusters. Reducing the number of 3D primitives, drastically speeds up pairwise matching.

3.2 Forming Ellipses

We model every cluster - pixel set - with an ellipse according to moments of the pixel coordinates. For an ellipse with major and minor radii a and b parallel to axes, we know:

$$\int x^2 dA = \frac{a^3 b \pi}{4} \tag{1}$$

$$\int y^2 dA = \frac{ab^3 \pi}{4} \tag{2}$$

$$\int xy dA = 0 \tag{3}$$

Rotating with α we get:

$$\begin{pmatrix} x' \\ y' \end{pmatrix} = \begin{bmatrix} c & -s \\ s & c \end{bmatrix} \begin{pmatrix} x \\ y \end{pmatrix} \tag{4}$$

$$tg2\alpha = \frac{2 \int x'y' dA}{\int y'^2 dA - \int x'^2 dA} \tag{5}$$

$$a^2 = 4 \frac{\int x'^2 dA + \int y'^2 dA + \frac{\int x'y' dA}{sc}}{\int 1 dA} \tag{6}$$

$$b = \frac{\int 1 dA}{a\pi} \tag{7}$$

Where $s = sin\alpha$, $c = cos\alpha$. We rejected too small and upright ellipses, these don't correspond to feet. Sample results can be seen in Fig. 2(c).

4 FINDING INTERSECTIONS

We back-projected ellipses in images to cones in scene space. Cones corresponding to a foot will intersect close to the location of foot. However, candidate pixels can also appear on arms or on foreground artifacts, and accidental intersections lead to false positives. Fig 3 shows such examples.

4.1 Forming Cones

We chose to describe a cone with a vertex C and three orthogonal vectors $\underline{u}$, $\underline{v}$ and $\underline{w}$, where $\underline{w}$ is the unit length direction vector of axis and $\underline{u}$, $\underline{v}$ are direction vectors of major and minor axes. Bevel angles are determined by the length of $\underline{u}$, $\underline{v}$ vectors. Cone consists of points $\underline{p}$ where

$$\left((\underline{p} - C)\underline{u}\right)^2 + \left((\underline{p} - C)\underline{v}\right)^2 \leq \left((\underline{p} - C)\underline{w}\right)^2, \tag{8}$$
$$(\underline{p} - C)\underline{w} \geq 0$$

For a calibrated camera, we know 3D position of points of image plane as well as the optical center O. Thus computing $\underline{w}$ is straightforward. $\underline{u}_i$, $\underline{v}_i$ point towards extremal points of ellipse in image plane, vector products ensure orthogonality of $\underline{u}$, $\underline{v}$, $\underline{w}$ vectors. Finally, $\underline{u}$ and $\underline{v}$ are scaled according to major and minor bevel angles so that (8) stands.

$$\underline{v} = \alpha \underline{u}_i \times \underline{w} \tag{9}$$

$$\underline{u} = \beta \underline{w} \times \underline{v} \tag{10}$$

4.2 Cone Matching

Intersection of cones is a complex body, but we found it is not necessary to know it exactly, just to measure the degree of intersecting. Thus we simplified matching in two ways:

(1) Feet are small in images, so bevel angles of cones will be small. Consequently, cones can be approximated with elliptical cylinders near intersection:

$$\left((\underline{p} - C)\underline{u}'\right)^2 + \left((\underline{p} - C)\underline{v}'\right)^2 < 1 \tag{11}$$

$$\underline{u}' = \underline{u}|\overrightarrow{CP_{close}}|, \quad \underline{v}' = \underline{v}|\overrightarrow{CP_{close}}| \tag{12}$$

Where $\overrightarrow{CP_{close}}$ is the distance of vertex closest to other cone's axis (see Fig. 4).

(2) Exact intersection of elliptic cylinders is still complex, therefore we tried to find an optimal point $\underline{p}$ in space, for which distance from cylinder axes is minimal - considering different major and minor radii.

Distance from axis - left side of (11) - is a linear function of $\underline{p}$, enabling us to write a linear equation
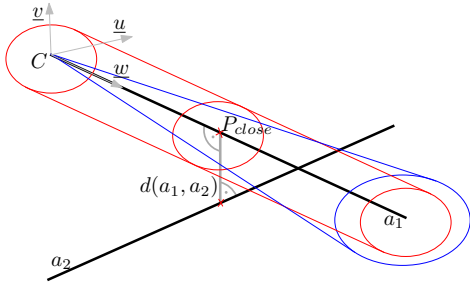
Figure 4: Elliptical cylinder for cone matching

system expressing $\underline{p}$ is on both axes (index refers to cylinders):

$$\begin{aligned}
\left((\underline{p} - C_1)\underline{u}_1'\right)^2 + \left((\underline{p} - C_1)\underline{v}_1'\right)^2 &= 0, \\
\left((\underline{p} - C_2)\underline{u}_2'\right)^2 + \left((\underline{p} - C_2)\underline{v}_2'\right)^2 &= 0
\end{aligned} \quad (13)$$

Equivalent to

$$\begin{bmatrix} \underline{u}_1'^T \\ \underline{v}_1'^T \\ \underline{u}_2'^T \\ \underline{v}_2'^T \end{bmatrix} \underline{p} = \begin{pmatrix} \underline{u}_1'C_1 \\ \underline{v}_1'C_1 \\ \underline{u}_2'C_2 \\ \underline{v}_2'C_2 \end{pmatrix} \quad (14)$$

$$A\underline{p} = \underline{b}$$

Of course, axes will practically never intersect, only approximate solution is possible. Solving subject to least square error is straightforward, as it minimizes sum of square distance from axes considering major and minor radii, and can be computed fast - we used pseudo inverse.

If $\underline{p}$ is outside any cylinder, we conclude cones are not intersecting, otherwise, they intersect and $\underline{p}$ is the position of the intersection - which we call match. We used error as the measure of degree of intersecting.

5 DETECTING FEET

A single object may result in multiple matches, close to each other. To avoid multiple detections, we merged close matches. We put merged set in the baricenter of matches, and we assigned a weight in a way, that the possibility of detection highly increases with the number of matches.

Matches - single or merged - with weights above a given threshold will form a detection. This threshold balances the tradeoff between precision and recall.

5.1 Reconstructing height Map

We found that in a dense crowd many false detections appear due to corrupt foreground mask or accidental intersections (as in Fig 3). However the height of these detections is quite random.
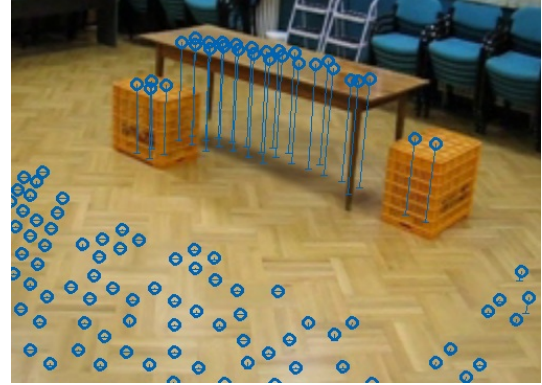

Figure 5: Generated height points for our test case.

Consequently these false positives appear as a noise, that can be suppressed using statistical filtering on a long video. Regions in space with many accumulated detections will determine ground, we call these height points. Height map consists of these height points.

The phrase height map is somewhat misleading, because at surface borders, it is possible to have multiple height points above each other, however in our tests this never occurred.

A sample height map of our non planar test case is shown in Fig 5. There are certain areas where few detections took place, this led to incomplete height map.

False positives tend to occur far from the ground, ignoring detections far from height map drastically improves performance.

6 EXPERIMENTS

Test sequences commonly used for multiview detection contain planar ground. Therefore we made test videos of a non planar ground to demonstrate capabilities of our method. We used four different consumer digital cameras with video capture function, and synchronized videos using a bouncing ball. We found that our algorithm performed well despite the different camera parameters, distortion and image quality.

We tested our algorithm on *EPFL terrace* (EPFL, 2011) (sample results can be seen in Fig 6), and *SZTAKI* (our own) sequences.

Detecting feet has advantages: **(1)** feet are always near ground, this enables us to compute and use height map, **(2)** in certain camera setups, feet are less likely to be occluded compared to whole bodies.

On the downside, accurate synchronization is mandatory, because slight time skew leads to errors comparable to the foot itself, preventing detection.

Figure 6: Corresponding frames from different cameras with the detected feet marked

Table 1: Statistical information on surfaces found in scene

surface	floor	box	table top
height	0cm	50cm	73cm
μ	0.6cm	49.7cm	73.9cm
σ	1.7cm	0.6cm	1.2cm
nr. of points	131	6	23
maximal error	10.7cm	1.4cm	3.2cm

6.1 Height Map Reconstruction

We found height map could be reconstructed precisely for both sequences. Height points from *EPFL* dataset fit well to a plane ($\sigma = 1.5cm$), height histogram is shown in Fig 7(a).

For our sequence, all three surfaces were found with high accuracy, measurements are summarized in Table 1. Few outliers lead to great maximal error in floor (see Fig 7(b)).

6.2 Detecting People

We tested our method using manually created ground truth information of feet positions. For a person, one or two legs can be specified, because sometimes only one foot is visible from more views.

Evaluation was carried out by matching detections to feet inside a region of interest (ROI). ROI is defined by a rectangle on floor so that every part is visible from at least three views (*EPFL* dataset provides ROI, for *SZTAKI* set we manually determined it).

Detection was accepted if it was not further than 25cm from a foot position - approximately the length of a foot. Unaccepted detections appear as false positives. As we detect persons, false negatives are people with none of their feet detected.

Detection threshold balances number of false positives/negatives. Therefore we measured precision-recall values in function of this threshold, Fig. 8 shows resulting ROC curves. Our experiments
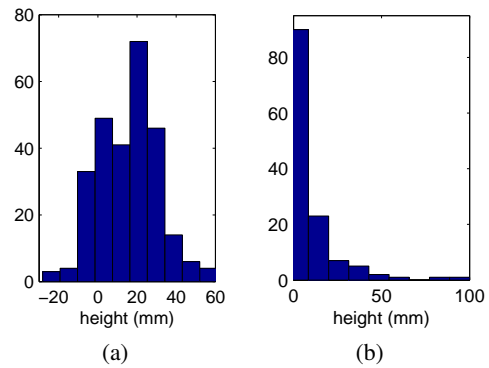

(a)   (b)

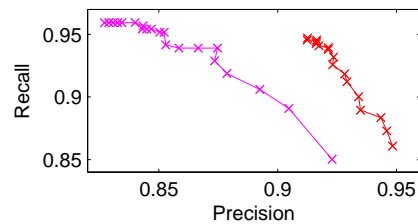Figure 7: Histogram of height of floor for (*a*) *EPFL* and (*b*) *SZTAKI* datasets.

Figure 8: ROC curve measured in function of detection threshold on terrace (red), and our test videos (magenta).

showed reflective surfaces were liable for worse results for our dataset.

With this evaluation method, our results became comparable to other multiview detection methods - where people are detected instead of feet. We found our results are comparable to SOA methods POM(Fleuret et al., 2008) and 3DMPP(Utasi and Benedek, 2011) (evaluated in (Utasi and Benedek, 2011) on *EPFL* and *PETS* datasets), in case of planar ground. Table 2 shows results.

6.3 Running Time

Table 3 shows average running times of steps of our algorithm (at video resolution of 360×288 for *EPFL* and 320×240 for *SZTAKI* sequences). As we can

Table 2: Comparison to SOA methods.

method	POM[a]	3DMPP[a]	Our method[b]
Precision	87.20	97.5	91.28
Recall	95.56	95.5	95.01

[a]evaluated on EPFL and PETS sequences (Utasi and Benedek, 2011), 395 frames with 1554 objects

[b]evaluated on EPFL sequence, 179 frames with 661 objects

Table 3: Average processing time of steps (4 views, single threaded implementation, 2.4GHz Core 2 Quad CPU).

	EPFL	*SZTAKI*
foreground detection	51.2ms	32.5ms
forming cones	3.43ms	4.87ms
matching/detection	907us	618us

see, real-time operation is possible even for single threaded implementation.

However, foreground detection and forming cones can be done independently for views, on multicore platforms or even on smart cameras. Matching and detection requires all cone information, but is extremely fast, real-time processing would still be possible with more views.

Many methods, including POM and 3DMPP, project parts or whole foreground masks to planes, which is computationally expensive, and distributing computation is not possible due to data dependencies.

7 CONCLUSION

We proposed a multiview-detection algorithm that retracts 3D position of people using multiple calibrated and synchronized views. In our case, unlike other algorithms, non-planar ground can be present. This is done by modeling possible positions of feet with 3D primitives, cones in scene space and searching for intersections of these cones.

For good precision, height map of ground should be known. Our method can compute height map on the fly, reaching high precision after a startup time.

After height map detection we measured precision and recall values comparable to SOA methods on commonly used data set. Our algorithm worked well also on our test videos we made to demonstrate capabilities of handling non-planar ground.

In the future we plan to examine tracking people by their leaning leg positions(Havasi et al., 2007).

REFERENCES

Benedek, C. and Szirányi, T. (2008). Bayesian foreground and shadow detection in uncertain frame rate surveillance videos. *IEEE Image Processing*, 17(4):608–621.

Berclaz, J., Fleuret, F., and Fua, P. (2006). Robust people tracking with global trajectory optimization. In *IEEE CVPR*, pages 744–750.

EPFL (2011). Multi-camera pedestrian videos. http://cvlab.epfl.ch/data/pom/.

Eshel, R. and Moses, Y. (2010). Tracking in a dense crowd using multiple cameras. *International Journal of Computer Vision*, 88:129–143.

Fleuret, F., Berclaz, J., Lengagne, R., and Fua, P. (2008). Multicamera people tracking with a probabilistic occupancy map. *IEEE Trans. Pattern Anal. Mach. Intell.*, 30(2):267–282.

Havasi, L. and Szlavik, Z. (2011). A method for object localization in a multiview multimodal camera system. In *CVPRW*, pages 96–103.

Havasi, L., Szlávik, Z., and Szirányi, T. (2007). Detection of gait characteristics for scene registration in video surveillance system. *IEEE Image Processing*, 16(2):503–510.

Iwase, S. and Saito, H. (2004). Parallel tracking of all soccer players by integrating detected positions in multiple view images. In *IEEE ICPR*, pages 751–754.

Jeong, K. and Jaynes, C. (2008). Object matching in disjoint cameras using a color transfer approach. *Machine Vision and Applications*, 19:443–455.

Khan, S. and Shah, M. (2006). A multiview approach to tracking people in crowded scenes using a planar homography constraint. In *ECCV 2006*, Lecture Notes in Computer Science, pages 133–146.

Khan, S. and Shah, M. (2009). Tracking multiple occluding people by localizing on multiple scene planes. *PAMI*, 31(3):505 –519.

Kim, K. and Davis, L. S. (2006). Multi-camera tracking and segmentation of occluded people on ground plane using search-guided particle filtering. In *ECCV*, pages 98–109.

Mittal, A. and Davis, L. (2001). Unified multi-camera detection and tracking using region-matching. In *IEEE Multi-Object Tracking*, pages 3 –10.

Mittal, A. and Davis, L. (2002). M2tracker: A multi-view approach to segmenting and tracking people in a cluttered scene using region-based stereo. In *ECCV 2002*, pages 18–33.

Utasi, Á. and Benedek, C. (2011). A 3-D marked point process model for multi-view people detection. In *IEEE CVPR*, pages 3385–3392.